Search for the doubly heavy baryon Ξ_{bc}^{+} decaying to $J/\psi\Xi_{c}^{+}$*

LHCb Collaboration†

Abstract: A first search for the $\Xi_{bc}^{+} \to J/\psi\Xi_{c}^{+}$ decay is performed by the LHCb experiment with a data sample of proton-proton collisions, corresponding to an integrated luminosity of 9 fb^{-1} recorded at centre-of-mass energies of 7, 8, and 13 TeV. Two peaking structures are seen with a local (global) significance of 4.3 (2.8) and 4.1 (2.4) standard deviations at masses of 6571 and 6694 MeV/c^2, respectively. Upper limits are set on the Ξ_{bc}^{+} baryon production cross-section times the branching fraction relative to that of the $B_c^{+} \to J/\psi D_s^{+}$ decay at centre-of-mass energies of 8 and 13 TeV, in the Ξ_{bc}^{+} and in the B_c^{+} rapidity and transverse-momentum ranges from 2.0 to 4.5 and 0 to 20 GeV/c, respectively. Upper limits are presented as a function of the Ξ_{bc}^{+} mass and lifetime.

Keywords: QCD, B physics, charm physics, spectroscopy

DOI: 10.1088/1674-1137/ace9c8

I. INTRODUCTION

Doubly heavy baryons consisting of two heavy quarks (b or c) and one light quark (u, d, or s) are expected within the quark model [1, 2]. In proton-proton (pp) collisions at the Large Hadron Collider, a possible model for production of these states is through gluon-gluon fusion, $g+g \to Q_1\overline{Q}_1 + Q_2\overline{Q}_2$ (Q denotes a heavy quark), a process that can be computed using perturbative quantum chromodynamics (QCD) [3–5]. The doubly heavy baryon is then formed via hadronisation where the two heavy quarks form a diquark which binds with a light quark. Other models exist, including production at the scale of the hard process, or production via non-perturbative effects such as colour reconnection. The measurement of the properties of these doubly heavy baryons provides insight into both their production mechanism and internal structure.

The observation and properties of the doubly heavy Ξ_{cc}^{++} (ccu) baryon have been firmly established by the LHCb collaboration [6–10], while the Ξ_{cc}^{+} (ccd) and Ω_{cc}^{+} (ccs) baryons have been searched for [11–13], and only hints of a signal were seen. The LHCb collaboration has also carried out searches for the neutral doubly heavy baryons, $\Xi_{bc}^{0}(bcd)$ [14] and $\Omega_{bc}^{0}(bcd)$ [15], but these states are yet to be observed.

To date, no search has been performed for the Ξ_{bc}^{+} baryon, a bound state with quark content bcu. This baryon is expected to have a mass in the range of 6700–7029 MeV/c^2 [16–35], while its lifetime is predicted to be between 240 and 607 fs [21, 31, 36–38]. The Ξ_{bc}^{+} production cross-section at a centre-of-mass energy of $\sqrt{s}$ =13 TeV is predicted to be about 16 nb [39] in the fiducial region $p_{\rm T} > 4$ GeV/c and $1.9 < \eta < 4.9$, where $p_{\rm T}$ is the momentum component transverse to the beam direction and η is the pseudorapidity.

This article presents the first search for the Ξ_{bc}^{+} baryon through its decay via the $J/\psi\Xi_{c}^{+}$ channel, with $J/\psi \to \mu^{+}\mu^{-}$ and $\Xi_{c}^{+} \to pK^{-}\pi^{+}$ final states, using pp collision data collected by the LHCb experiment at centre-of-mass energies of 7, 8, and 13 TeV, corresponding to integrated luminosities of 1, 2, and 6 fb^{-1}, respectively.

The search for this decay is advantageous over the previous Ξ_{bc}^{0} searches in several ways. First, the Ξ_{bc}^{+} baryon is expected to have a larger lifetime than that of the

Received 19 April 2022; Accepted 23 June 2022; Published online 24 July 2023

* The project support from CERN and from the national agencies: CAPES, CNPq, FAPERJ and FINEP (Brazil); MOST and NSFC (China); CNRS/IN2P3 (France); BMBF, DFG and MPG (Germany); INFN (Italy); NWO (Netherlands); MNiSW and NCN (Poland); MEN/IFA (Romania); MICINN (Spain); SNSF and SER (Switzerland); NASU (Ukraine); STFC (United Kingdom); DOE NP and NSF (USA). We acknowledge the computing resources that are provided by CERN, IN2P3 (France), KIT and DESY (Germany), INFN (Italy), SURF (Netherlands), PIC (Spain), GridPP (United Kingdom), CSCS (Switzerland), IFIN-HH (Romania), CBPF (Brazil), Polish WLCG (Poland) and NERSC (USA). Individual groups or members have received support from ARC and ARDC (Australia); Minciencias (Colombia); AvH Foundation (Germany); EPLANET, Marie Sklodowska-Curie Actions and ERC (European Union); A*MIDEX, ANR, IPhU and Labex P2IO, and Région Auvergne-Rhône-Alpes (France); Key Research Program of Frontier Sciences of CAS, CAS PIFI, CAS CCEPP, Fundamental Research Funds for the Central Universities, and Sci. & Tech. Program of Guangzhou (China); GVA, XuntaGal, GENCAT and Prog. Atracción Talento, CM (Spain); SRC (Sweden); the Leverhulme Trust, the Royal Society and UKRI (United Kingdom).

† Authors are listed at the end of this paper.

Ξ_{bc}^0 baryon [21, 31, 36–38], which leads to a larger selection efficiency as the lifetime information is used to suppress background from primary pp interactions. Second, the mode studied here uses $J/\psi \to \mu^+\mu^-$ decays, which typically have a selection efficiency three times larger than the fully hadronic modes used in the previous Ξ_{bc}^0 searches. Last, the modes used in the Ξ_{bc}^0 analyses involved suppressed $b \to u$ or $b \to s$ transitions, or W-exchange diagrams. Here the decay to the $J/\psi\Xi_c^+$ final state involves a colour-suppressed $b \to c$ transition, with a decay amplitude that is less likely to be suppressed, as shown in Fig. 1.

To reduce systematic uncertainties, the Ξ_{bc}^+ production cross-section times the $\Xi_{bc}^+ \to J/\psi\Xi_c^+$ branching fraction is measured relative to that of the normalisation mode $B_c^+ \to J/\psi D_s^+$ with $J/\psi \to \mu^+\mu^-$ and $D_s^+ \to K^+K^-\pi^+$ decays. Specifically, the quantity $\mathcal{R}$ is defined as

$$\mathcal{R} = \frac{\sigma(\Xi_{bc}^+)\times\mathcal{B}(\Xi_{bc}^+ \to J/\psi\Xi_c^+)\times\mathcal{B}(\Xi_c^+ \to pK^-\pi^+)}{\sigma(B_c^+)\times\mathcal{B}(B_c^+ \to J/\psi D_s^+)\times\mathcal{B}(D_s^+ \to K^+K^-\pi^+)}, \quad (1)$$

where $\sigma(\Xi_{bc}^+)$ and $\sigma(B_c^+)$ are the production cross-sections of Ξ_{bc}^+ and B_c^+ hadrons, respectively, and $\mathcal{B}$ is the branching fraction of the corresponding decay. The ratio $\mathcal{R}$ is measured in the rapidity range $2.0 < y < 4.5$ and in the $p_{\rm T}$ region from 0 to 20 GeV/c. Measurements of $\mathcal{R}$ are reported for the $\sqrt{s} = 8$ and 13 TeV data sets collected in 2012 and 2016–2018, corresponding to integrated luminosities of 2 and 5.4 fb^{-1}, respectively. The 2011 data sample taken with a centre-of-mass energy of 7 TeV is small, and it is not used in the production rate measurement.

The ratio $\mathcal{R}$ is evaluated as

$$\mathcal{R} = \frac{\varepsilon_{\rm norm}}{\varepsilon_{\rm sig}}\frac{N_{\rm sig}}{N_{\rm norm}} \equiv \alpha N_{\rm sig}, \quad (2)$$

where $\varepsilon_{\rm sig}$ and $\varepsilon_{\rm norm}$ are the total efficiencies of the Ξ_{bc}^+ signal and B_c^+ normalisation decay modes, $N_{\rm sig}$ and $N_{\rm norm}$ are the corresponding signal yields, and the derived quantity α is the single-event sensitivity.

An estimate for $\mathcal{R}$ can be obtained by assuming that the ratio of production cross-sections $\sigma(\Xi_{bc}^+)/\sigma(B_c^+)$ is about 0.4 [39–41], $\mathcal{B}(\Xi_{bc}^+ \to J/\psi\Xi_c^+) \sim 1/3 \cdot \mathcal{B}(B_c^+ \to J/\psi D_s^+)$ due to colour suppression, $\mathcal{B}(\Xi_c^+ \to pK^-\pi^+) = (0.62 \pm 0.30)\%$ [42, 43], $\mathcal{B}(D_s^+ \to K^+K^-\pi^+) = (5.39 \pm 0.15)\%$ [44], and assuming an efficiency ratio $\varepsilon_{\rm sig}/\varepsilon_{\rm norm} \sim 1$. With these inputs, the value $\mathcal{R} \sim 0.015$ is obtained. With 1100 $B_c^+ \to J/\psi D_s^+$ candidates observed in the full data set collected by the LHCb experiment [45], approximately 15 reconstructed $\Xi_{bc}^+ \to J/\psi\Xi_c^+$ signal decays are expected in the LHCb detector acceptance.

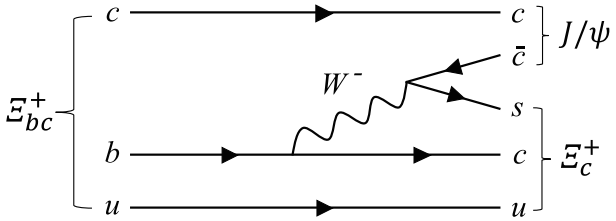

Fig. 1. Example leading-order Feynman diagram for the $\Xi_{bc}^+ \to J/\psi\Xi_c^+$ decay.

II. LHCb DETECTOR AND SIMULATION

The LHCb detector [46, 47] is a single-arm forward spectrometer covering the range $2 < \eta < 5$, designed for the study of particles containing b or c quarks. It includes a high-precision tracking system consisting of a silicon-strip vertex detector surrounding the pp interaction region [48], a large-area silicon-strip detector located upstream of a dipole magnet with a bending power of about 4 Tm, and three stations of silicon-strip detectors and straw drift tubes [49, 50] placed downstream of the magnet. The tracking system provides a measurement of the momentum, p, of charged particles with a relative uncertainty that varies from 0.5% at low p to 1.0% at 200 GeV/c. The minimum distance of a track to a primary pp collision vertex (PV), the impact parameter (IP), is measured with a resolution of $(15 + 29/p_{\rm T})$ μm, where $p_{\rm T}$ is expressed in GeV/c. Different types of charged hadrons are distinguished using information from two ring-imaging Cherenkov detectors [51]. Photons, electrons and hadrons are identified by a calorimeter system consisting of scintillating-pad and preshower detectors, an electromagnetic and a hadronic calorimeter. Muons are identified by a system composed of alternating layers of iron and multiwire proportional chambers [52]. The online event selection is performed by a trigger [53], which consists of a hardware stage, based on information from the calorimeter and muon systems, followed by a two-level software stage, which applies a full event reconstruction.

Simulation of signal and normalisation modes is required to model the effects of the detector acceptance and the imposed selection requirements. In the simulation, pp collisions are generated using Pythia 8 [54] with a specific LHCb configuration [55]. A dedicated generator, GenXicc 2.0 [5], is used to simulate the doubly heavy baryon production, and is interfaced to Pythia 8 to provide underlying event, parton shower, and hadronisation generation. Decays of unstable particles are described by EvtGen [56], in which final-state radiation is generated using Photos [57]. The interaction of the generated particles with the material of the detector, and its response, are simulated using the Geant4 toolkit [58] as described in Ref. [59]. The simulated Ξ_{bc}^+ events are generated with a mass of 6900 MeV/c^2 and a lifetime of 400 fs, and samples with different mass and lifetime hypotheses

are obtained using a weighting technique, described in Sec. VII. The Ξ_{bc}^+ baryon is assumed to decay uniformly within the allowed phase space.

III. RECONSTRUCTION AND SELECTION

For both the Ξ_{bc}^+ signal and the B_c^+ normalisation mode, J/ψ candidates are reconstructed from $\mu^+\mu^-$ pairs. In the online event selection the J/ψ candidates are required to pass dedicated trigger requirements. At the hardware stage at least one high-$p_{\rm T}$ muon is required. In the subsequent software stage, a pair of oppositely charged muon candidates is required to originate from a common vertex that is displaced from any PV and to have an invariant mass$m(\mu^+\mu^-)$ in a wide window around the J/ψ mass.

In the offline selection, J/ψ candidates are formed by two oppositely charged tracks identified as muons, with $m(\mu^+\mu^-)$ in the range between 3040 and 3140 MeV/c^2, and that are required to be consistent with a common vertex that is significantly displaced from any PV. For the Ξ_{bc}^+ signal mode, the Ξ_c^+ candidates are reconstructed in the $pK^-\pi^+$ final state. The three tracks, identified as a proton, kaon, and pion, are required to be inconsistent with originating from any PV in the event and form a common vertex with good fit quality. The reconstructed mass of the Ξ_c^+ candidates is required to be within ±15 MeV/c^2 of the known Ξ_c^+ mass [44], which corresponds to about 2.5 times the mass resolution. For the B_c^+ normalisation mode, the D_s^+ candidates are reconstructed in the $K^+K^-\pi^+$ final state, and selected in the same way as the Ξ_c^+ candidates, apart from different particle identification (PID) requirements. The J/ψ and Ξ_c^+ (D_s^+) candidates are then required to form a common vertex with a good fit quality to reconstruct the Ξ_{bc}^+ (B_c^+) candidate. Each Ξ_{bc}^+ (B_c^+) is associated to the PV in the event for which $\chi^2_{\rm IP}$ is the smallest, where $\chi^2_{\rm IP}$ is the difference in χ^2 of the PV fit with and without the Ξ_{bc}^+ (B_c^+) included in the PV fit. The Ξ_{bc}^+ (B_c^+) candidate is required to have a trajectory that points back to its associated PV.

A boosted decision tree (BDT) algorithm [60, 61] implemented in the TMVA package [62] is applied to both the signal and the normalisation candidates to further improve the purity of the samples. To train this classifier, simulated Ξ_{bc}^+ baryon decays are used as signal proxy and candidates lying in the upper $J/\psi\Xi_c^+$ mass sideband, with $m(J/\psi\Xi_c^+)$ in the range of 8000–8500 MeV/c^2, are used to model the background. The BDT algorithm uses kinematic and vertex-topology variables that show a good discrimination power between signal and background samples. The variables include: the $\chi^2_{\rm IP}$, p and $p_{\rm T}$ of all particles; PID variables for the final state particles; the flight-distance χ^2 between the PV and the decay vertex; and the vertex fit quality of the J/ψ, Ξ_c^+ and Ξ_{bc}^+ candidates. The flight-distance χ^2 is defined as the χ^2 of the hypothesis that the decay vertex of the candidate coincides with its associated PV.

The threshold of the BDT response is set by maximising the figure of merit [63] $\varepsilon/(\beta/2+\sqrt{N_B})$, where ε is the signal efficiency estimated from simulation, β corresponds to the number of standard deviations in a Gaussian significance test, which is taken as 5, and N_B is the number of background candidates determined in the upper sideband and extrapolated to the signal region. The performance of the BDT classifier is tested and found to be stable against the Ξ_{bc}^+ lifetime in the range from 300 to 500 fs. The same BDT selection is applied to the normalisation mode, with the PID requirements changed accordingly.

IV. YIELD MEASUREMENTS

The invariant-mass distributions of selected Ξ_{bc}^+ and B_c^+ candidates in the full data sample are shown in Figs. 2 and 3, respectively. To improve the mass resolution of the Ξ_{bc}^+ (B_c^+) candidates, the $J/\psi\Xi_c^+$ ($J/\psi D_s^+$) invariant mass is

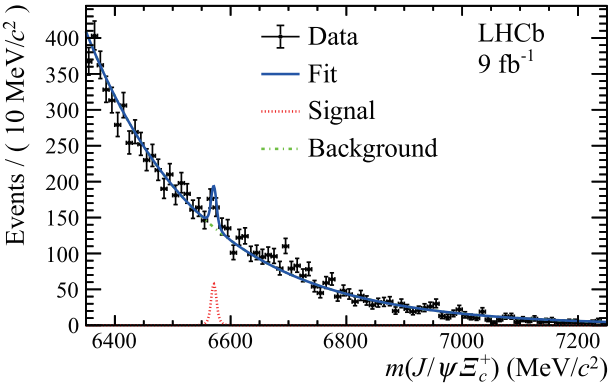

Fig. 2. (color online) Mass $m(J/\psi\Xi_c^+)$ distribution of selected Ξ_{bc}^+ candidates for the full data set. The fit (blue solid line) with the largest local significance at the mass of 6571 MeV/c^2 is superimposed.

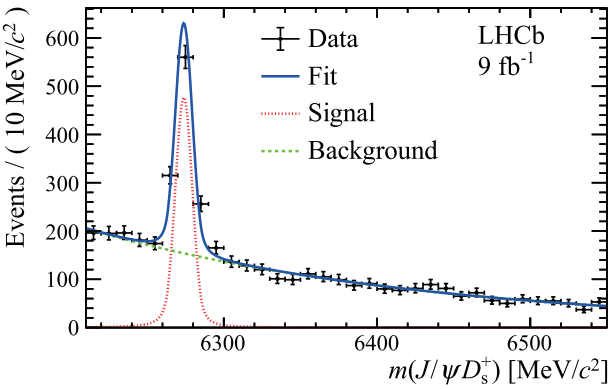

Fig. 3. (color online) Mass $m(J/\psi D_s^+)$ distribution of selected B_c^+ candidates for the full data set. The fit (blue solid line) is superimposed.

calculated by constraining the J/ψ and Ξ_c^+ (D_s^+) masses to their known values [44] and the Ξ_{bc}^+ (B_c^+) candidates to originate from their associated PV [64].

The Ξ_{bc}^+ signal yield is determined from an unbinned maximum-likelihood fit to the $J/\psi\Xi_c^+$ mass distribution. The signal is described by a double-sided Crystal Ball (DSCB) function [65] comprising a Gaussian core with power-law tails on both sides, where the tail parameters depend on the mass resolution, while the combinatorial background is described by an exponential function. The dependence of the mass resolution on the Ξ_{bc}^+ mass is determined from simulation. The mass resolution varies from about 4 MeV/c^2 at a Ξ_{bc}^+ mass of 6400 to 7 MeV/c^2 at 7100 MeV/c^2. The mass region of interest from 6430 to 7120 MeV/c^2 is scanned in 3 MeV/c^2 steps, to search for any significant structures.

The local significance of a signal peak is quantified with a p-value, which is calculated from the likelihood ratio between the background-plus-signal and the background-only hypotheses [66]. The local p-value is plotted in Fig. 4 as a function of $m(J/\psi\Xi_c^+)$, showing a dip around 6571 MeV/c^2, which has the largest local significance, expressed in number of standard deviations (σ), corresponding to 4.3σ. Another dip is seen around 6694 MeV/c^2, with a local significance of 4.1σ. The fit results for the two mass peaks at 6571 and 6694 MeV/c^2 are shown in Figs. 2 and 5, and the signal yield is 75 ± 19 and 58 ± 16, respectively. The global significance is evaluated using pseudoexperiments, by taking into account the look-elsewhere effect [67] in the mass range from 6430 to 7120 MeV/c^2, and is estimated to be 2.8σ and 2.4σ for the two mass peaks at 6571 and 6694 MeV/c^2, respectively. As no excess above 3σ is observed, upper limits on the production ratios are set for the data samples with centre-of-mass energies of $\sqrt{s} = 8$ and 13 TeV.

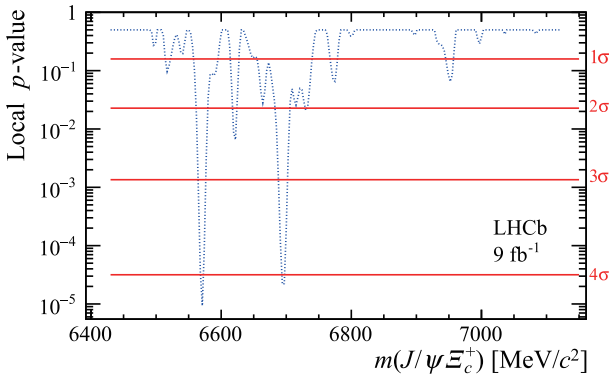

Fig. 4. (color online) Local p-value in the $m(J/\psi\Xi_c^+)$ range 6430–7120 MeV/c^2.

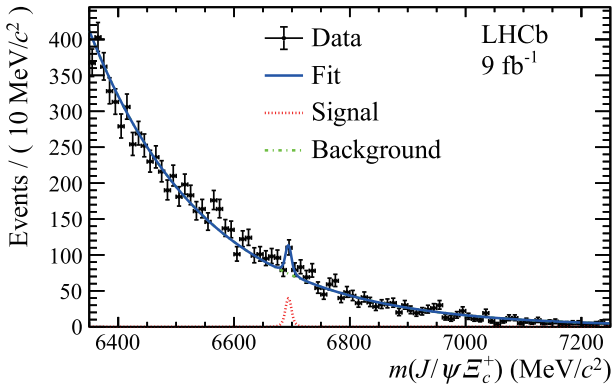

Fig. 5. (color online) Mass $m(J/\psi\Xi_c^+)$ distribution of selected Ξ_{bc}^+ candidates for the full data set. The fit (blue solid line) with the Second largest local significance at the mass of 6694 MeV/c^2 is superimposed.

The B_c^+ signal yield is determined from an unbinned maximum-likelihood fit to the $m(J/\psi D_s^+)$ distribution. The B_c^+ signal is described by a DSCB function with the tail parameters depending on the mass resolution [45], while the combinatorial background is described by an exponential function. The fit to the full data set is shown in Fig. 3. A total of 706 ± 38 $B_c^+ \to J/\psi D_s^+$ signal decays are selected. The signal yields used in the measurement of $\mathcal{R}$ are summarised in Table 1.

Table 1. Efficiency ratios $\varepsilon_{\rm norm}/\varepsilon_{\rm sig}$ between the normalisation and signal modes, signal yields of the normalisation mode $N_{\rm norm}$, and the single-event sensitivity α, for the default mass and lifetime of the Ξ_{bc}^+ baryon, 6900 MeV/c^2 and 400 fs, respectively. Uncertainties are statistical only.

Data sample	$\varepsilon_{\rm norm}/\varepsilon_{\rm sig}$	$N_{\rm norm}$	α
2012 ($\sqrt{s}$= 8 TeV)	1.316 ± 0.013	75 ± 13	0.018 ± 0.003
2016 ($\sqrt{s}$=13 TeV)	1.207 ± 0.007	177 ± 20	0.0068 ± 0.0008
2017 ($\sqrt{s}$=13 TeV)	1.202 ± 0.006	193 ± 20	0.0062 ± 0.0006
2018 ($\sqrt{s}$=13 TeV)	1.222 ± 0.006	220 ± 21	0.0056 ± 0.0005

V. EFFICIENCY RATIOS

The efficiency ratio between the B_c^+ and Ξ_{bc}^+ modes, defined as $\varepsilon_{\rm norm}/\varepsilon_{\rm sig}$, is determined from simulation, along with corrections to account for small residual differences between data and simulation. The signal efficiency depends upon the assumed mass and lifetime of the Ξ_{bc}^+ baryon. Simulated events are generated with a Ξ_{bc}^+ mass of 6900 MeV/c^2 and a lifetime $\tau(\Xi_{bc}^+) = 400$ fs, labelled here as default. The tracking and PID efficiencies for both the signal and normalisation modes are corrected using calibration data samples [68–70]. The PID efficiency correction is applied by resampling the distributions of PID observables in simulation to match those in data for the variables used in the selection and in the BDT classifier before computing the efficiency. The efficiency ratio and the single-event sensitivity at the default Ξ_{bc}^+ mass and lifetime are summarised in Table 1 together with the signal yield of the normalisation mode, used in computing the single-event sensitivity.

The efficiency ratio for other lifetime values are obtained by weighting the simulated events to reproduce lifetime hypotheses from 300 to 500 fs in 50 fs steps. An event-by-event weight is calculated as

$$w = \frac{(1/\tau)\cdot\exp(-t/\tau)}{(1/\tau_0)\cdot\exp(-t/\tau_0)}, \quad (3)$$

where t is the Ξ_{bc}^+ decay time, τ is the new lifetime and τ_0 is the default lifetime. The total efficiency is found to have a linear dependence on the Ξ_{bc}^+ lifetime. The value and uncertainty in the single-event sensitivity α are provided for each lifetime hypothesis and for each data-taking period (Table 2). The efficiency could also depend on the Ξ_{bc}^+ baryon mass hypothesis in the simulation, since it affects the kinematic distributions of the decay products. To assess this effect, large samples of simulated events are generated with alternative mass hypotheses in the range 6400–7050 MeV/c^2 in 50 MeV/c^2 steps. These samples are used to weight the $p_{\rm T}$ distributions of the final-state particles in the fully simulated Ξ_{bc}^+ decay to match those of the other mass hypotheses, and the efficiency is then recalculated. A very small dependence on the Ξ_{bc}^+ mass, a 0.4% relative variation of the signal efficiency due to this weighting, is observed and considered as a systematic uncertainty.

Table 2. Single-event sensitivity α in units of 10^{-3} for different lifetime hypotheses of the Ξ_{bc}^+ baryon for different data taking periods. Uncertainties are due to the limited size of the simulated samples and the statistical uncertainties in the measured B_c^+ yields.

Data sample	300 fs	350 fs	400 fs	450 fs	500 fs
2012 ($\sqrt{s}$= 8 TeV)	22 ± 4	20 ± 3	18 ± 3	16 ± 2	15 ± 2
2016 ($\sqrt{s}$=13 TeV)	8.4 ± 0.9	7.5 ± 0.8	6.8 ± 0.8	6.3 ± 0.7	5.9 ± 0.6
2017 ($\sqrt{s}$=13 TeV)	7.7 ± 0.7	6.8 ± 0.7	6.2 ± 0.6	5.7 ± 0.6	5.4 ± 0.5
2018 ($\sqrt{s}$=13 TeV)	6.9 ± 0.6	6.2 ± 0.6	5.6 ± 0.5	5.2 ± 0.5	4.9 ± 0.4

VI. SYSTEMATIC UNCERTAINTIES

Systematic uncertainties affecting the measurement of $\mathcal{R}$ arise from the PID efficiency corrections, the track reconstruction efficiency, the difference in the $\Xi_c^+ \to pK^-\pi^+$ Dalitz distribution between data and simulation, the variation of the efficiency with respect to the Ξ_{bc}^+ mass, the mass resolution used in the fit to the Ξ_{bc}^+ mass spectrum, and the fit model assumed to evaluate the normalisation yield. The total systematic uncertainty is calculated as the quadratic sum of each individual uncertainty presented in Table 3, assuming no correlation between the contributions.

The largest systematic uncertainty is due to the PID efficiency correction. There are several sources of systematic uncertainty associated to this correction, mainly due to the limited size of the calibration samples, the assumption of no correlations between PID variables of each final state particle, and limitations in the method used to correct the PID variables. The largest contribution to the PID efficiency correction arises from the comparison between the efficiency obtained with the PID variables resampled assuming no correlations between the PID variables for each final state particle, and an alternative correction method that takes into account such correlations. This alternative method requires corrections in a higher number of dimensions of phase space, and can suffer from statistical fluctuations due to limited size of the calibration samples. This comparison gives a 3.6% contribution to the PID efficiency correction uncertainty. Summing all the contributions in quadrature, the total systematic uncertainty associated to the PID efficiency correction is 4%.

Table 3. Systematic uncertainties on the measurement of the production ratio, $\mathcal{R}$.

Source	$\mathcal{R}$ (%)
PID	4.0
Tracking	0.8
$\Xi_c^+ \to pK^-\pi^+$ Dalitz distribution	0.5
Ξ_{bc}^+ mass	0.4
Mass resolution	1.5
B_c^+ signal shape	0.2
Total systematic uncertainty	4.4

Two sources contribute to the systematic uncertainty associated to the tracking efficiency. The first uncertainty is statistical, arising from the limited size of the samples used to derive the efficiency correction. The second is due to hadronic interactions with the detector material [68]. Considering that two out of the three final-state hadrons in the signal and the normalisation modes are common, the effect cancels out in the ratio except for the proton coming from the Ξ_c^+ decay and the positively charged kaon from the D_s^+ decay. These two uncertainties are added in quadrature and the total systematic uncertainty due to the tracking efficiency is 0.8%.

The uncertainty contribution due to the $\Xi_c^+ \to pK^-\pi^+$ decay comes from an imperfect modelling of the Dalitz shape in the simulation. A new signal efficiency is obtained using a weighting technique to match the simulated Dalitz distribution with the one from data, and the resulting difference of 0.5% is taken as a systematic uncertainty.

As described earlier, the Ξ_{bc}^+ selection efficiency is found to depend on the Ξ_{bc}^+ mass at a level of 0.4%, which is neglected in the efficiency ratio, and is taken as

a systematic uncertainty. The uncertainty coming from possible variations of the mass resolution, used in the $m(J/\psi\Xi_c^+)$ fit, are obtained by varying the mass resolution by $\pm 10\%$. The largest difference between the local significance from the p-value scan obtained with different mass resolutions, 1.5%, is taken as a systematic uncertainty. The signal yield of the normalisation mode is affected by the fit model. This is evaluated by considering a sum of two Gaussian functions with the same mean but different resolutions, rather than the default DSCB function. The difference between the two measured yields, 0.2%, is taken as a systematic uncertainty. The total systematic uncertainty on the measurement of the production ratio $\mathcal{R}$ is 4.4%.

VII. RESULTS AND SUMMARY

The search for the Ξ_{bc}^+ baryon shows no significant signal, and therefore upper limits at the 95% credibility level (CL) are set. The upper limits include the systematic uncertainties, obtained by convolving the likelihood profile $\mathcal{L}(\mathcal{R})$ with a Gaussian distribution whose width is given by the quadratic sum of the uncertainty in the single-event sensitivity and the systematic uncertainties. The likelihood profile $\mathcal{L}(\mathcal{R})$ is calculated by setting different Ξ_{bc}^+ mass hypotheses in the fit to the $J/\psi\Xi_c^+$ invariant-mass distribution, with a step of 3 MeV/c^2. The upper limit at 95% CL is defined as the value of $\mathcal{R}$ at which the integral of the likelihood profile equals 95% of its total area.

The resulting 95% CL upper limits on $\mathcal{R}$ as a function of assumed Ξ_{bc}^+ mass are shown in Figs. 6 and 7 for the $\sqrt{s} = 8$ and 13 TeV data samples, respectively. The results are restricted to the kinematic region $2.0 < y < 4.5$ and $0 < p_{\rm T} < 20\,{\rm GeV}/c$. Upper limits at several different lifetimes of Ξ_{bc}^+ (300, 350, 400, 450 and 500 fs) are also shown at each centre-of-mass energy. The upper limits are set assuming that the kinematic distributions of the Ξ_{bc}^+ baryon follow those of the GenXicc 2.0 model [5] and that the Ξ_{bc}^+ baryon decays uniformly within the available phase space.

In summary, a first search for the Ξ_{bc}^+ baryon using $\Xi_{bc}^+ \to J/\psi\Xi_c^+$ decays is reported by the LHCb experiment using a pp collision data sample corresponding to an integrated luminosity of 9 fb^{-1}, recorded at centre-of-mass energies of 7, 8, and 13 TeV. The most significant peaks in the mass region considered correspond to local (global) significance of 4.3σ (2.8σ) and 4.1σ (2.4σ) at 6571 and 6694 MeV/ c^2. Thus, there is no evidence for the Ξ_{bc}^+ baryon with the current data sample. The 95% CL upper limits on the relative production rate $\mathcal{R}$ of Ξ_{bc}^+ baryons relative to the B_c^+ meson, are reported at $\sqrt{s}$=8 and 13 TeV in the kinematic region $2.0 < y < 4.5$ and transverse momentum $0 < p_{\rm T} < 20\,{\rm GeV}/c$ for a range of possible Ξ_{bc}^+ lifetimes.

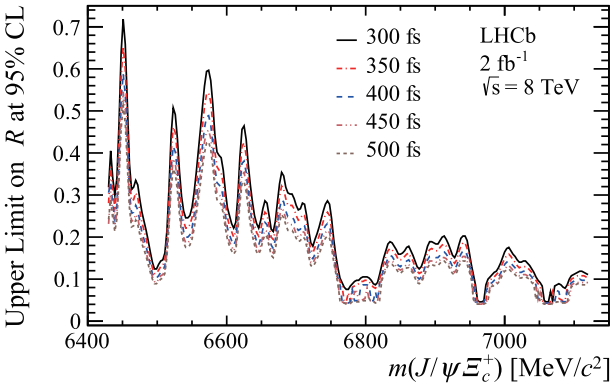

Fig. 6. (color online) Upper limits on $\mathcal{R}$ at 95% CL as a function of $m(J/\psi\Xi_c^+)$ for five Ξ_{bc}^+ lifetime hypotheses (300, 350, 400, 450 and 500 fs) at a centre-of-mass energy of $\sqrt{s} = 8$ TeV. The curves from top to bottom correspond to lifetime hypotheses from 300 fs to 500 fs, respectively.

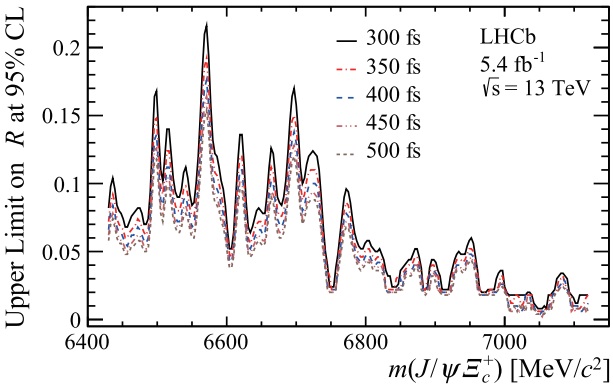

Fig. 7. (color online) Upper limits on $\mathcal{R}$ at 95% CL as a function of $m(J/\psi\Xi_c^+)$ for five Ξ_{bc}^+ lifetime hypotheses (300, 350, 400, 450 and 500 fs) at a centre-of-mass energy of $\sqrt{s} =$ 13 TeV. The curves from top to bottom correspond to lifetime hypotheses from 300 fs to 500 fs, respectively.

In the region favoured by most theoretical models (6700–7029 MeV/c^2), the limits on $\mathcal{R}$ for the 13 TeV data sample are close to the rough estimate of 0.015 discussed previously in Sec. I. With the larger data samples anticipated in the future running of the LHCb experiment and the inclusion of additional decay modes there is potential for evidence or discovery of the Ξ_{bc}^+ baryon in the future.

ACKNOWLEDGEMENTS

We express our gratitude to our colleagues in the CERN accelerator departments for the excellent performance of the LHC. We thank the technical and administrative staff at the LHCb institutes. We are indebted to the communities behind the multiple open-source software packages on which we depend.

References

[1] M. Gell-Mann, Phys. Lett. **8**, 214 (1964)
[2] G. Zweig, CERN-TH-401, CERN, Geneva, 1964; G. Zweig, CERN-TH-412, CERN, Geneva, 1964
[3] J. P. Ma and Z. G. Si, Phys. Lett. B **568**, 135 (2003), arXiv:hep-ph/0305079
[4] C.-H. Chang, J.-P. Ma, C.-F. Qiao *et al.*, J. Phys. G **34**, 845 (2007), arXiv:hep-ph/0610205
[5] C.-H. Chang, J.-X. Wang, and X.-G. Wu, Comput. Phys. Commun. **181**, 1144 (2010), arXiv:0910.4462
[6] R. Aaij *et al.* (LHCb collaboration), Phys. Rev. Lett. **119**, 112001 (2017), arXiv:1707.01621
[7] R. Aaij *et al.* (LHCb collaboration), Phys. Rev. Lett. **121**, 052002 (2018), arXiv:1806.02744
[8] R. Aaij *et al.* (LHCb collaboration), JHEP **10**, 124 (2019), arXiv:1905.02421
[9] R. Aaij *et al.* (LHCb collaboration), Chin. Phys. C **44**, 022001 (2020), arXiv:1910.11316
[10] R. Aaij *et al.* (LHCb collaboration), JHEP **02**, 049 (2020), arXiv:1911.08594
[11] R. Aaij *et al.* (LHCb collaboration), Sci. China Phys. Mech. Astron. **63**, 221062 (2020), arXiv:1909.12273
[12] R. Aaij *et al.* (LHCb collaboration), JHEP **12**, 107 (2021), arXiv:2109.07292
[13] R. Aaij *et al.* (LHCb collaboration), Sci. China Phys. Mech. Astron. **64**, 101062 (2021), arXiv:2105.06841
[14] R. Aaij *et al.* (LHCb collaboration), JHEP **11**, 095 (2020), arXiv:2009.02481
[15] R. Aaij *et al.* (LHCb collaboration), Chin. Phys. C **45**, 093002 (2021), arXiv:2104.04759
[16] W. Ponce, Phys. Rev. D **19**, 2197 (1979)
[17] R. Roncaglia, D. B. Lichtenberg, and E. Predazzi, Phys. Rev. D **52**, 1722 (1995), arXiv:hep-ph/9502251
[18] B. Silvestre-Brac, Prog. Part. Nucl. Phys. **36**, 263 (1996)
[19] D. B. Lichtenberg, R. Roncaglia, and E. Predazzi, Phys. Rev. D **53**, 6678 (1996), arXiv:hep-ph/9511461
[20] D. Ebert *et al.*, Z. Phys. C **76**, 111 (1997), arXiv:hep-ph/9607314
[21] V. V. Kiselev *et al.*, Phys. Usp. **45**, 455 (2002), arXiv: hep-ph/0103169, [Usp. Fiz. Nauk **172**, 497 (2002)]
[22] D. Ebert, R. N. Faustov, V. O. Galkin, Phys. Rev. D **66**, 014008 (2002), arXiv:hep-ph/0201217
[23] D.-H. He *et al.*, Phys. Rev. D **70**, 094004 (2004), arXiv:hep-ph/0403301
[24] C. Albertus, E. Hernandez, J. Nieves *et al.*, Eur. Phys. J. A **32**, 183 (2007), arXiv: hep-ph/0610030, [Erratum: Eur. Phys. J. A **36**, 119 (2008)]
[25] W. Roberts and M. Pervin, Int. J. Mod. Phys. A **23**, 2817 (2008), arXiv:0711.2492
[26] J.-R. Zhang and M.-Q. Huang, Phys. Rev. D **78**, 094007 (2008), arXiv:0810.5396
[27] S. M. Gerasyuta and E. E. Matskevich, Int. J. Mod. Phys. E **18**, 1785 (2009), arXiv:0803.3497
[28] F. Giannuzzi, Phys. Rev. D **79**, 094002 (2009), arXiv:0902.4624
[29] M.-H. Weng, X.-H. Guo, and A. W. Thomas, Phys. Rev. D **83**, 056006 (2011), arXiv:1012.0082
[30] T. M. Aliev, K. Azizi, and M. Savci, Nucl. Phys. A **895**, 59 (2012), arXiv:1205.2873
[31] M. Karliner and J. L. Rosner, Phys. Rev. D **90**, 094007 (2014), arXiv:1408.5877
[32] Z. S. Brown, W. Detmold, S. Meinel *et al.*, Phys. Rev. D **90**, 094507 (2014), arXiv:1409.0497
[33] X.-Z. Weng, X.-L. Chen, and W.-Z. Deng, Phys. Rev. D **97**, 054008 (2018), arXiv:1801.08644
[34] Q. Li, C.-H. Chang, S.-X. Qin *et al.*, Eur. Phys. J. C **82**, 60 (2022), arXiv:2112.10966
[35] Z.-G. Wang and Q. Xin, Int. J. Mod. Phys. A **37**, 2250074 (2022), arXiv:2202.03828
[36] V. V. Kiselev, A. K. Likhoded, and A. I. Onishchenko, Eur. Phys. J. C **16**, 461 (2000), arXiv:hep-ph/9901224
[37] A. V. Berezhnoy, A. K. Likhoded, and A. V. Luchinsky, Phys. Rev. D **98**, 113004 (2018), arXiv:1809.10058
[38] H.-Y. Cheng and F. Xu, Phys. Rev. D **99**, 073006 (2019), arXiv:1903.08148
[39] J.-W. Zhang *et al.*, Phys. Rev. D **83**, 034026 (2011), arXiv:1101.1130
[40] C.-H. Chang and X.-G. Wu, Eur. Phys. J. C **38**, 267 (2004), arXiv:hep-ph/0309121
[41] Y.-N. Gao *et al.*, Chin. Phys. Lett. **27**, 061302 (2010)
[42] Y. B. Li *et al.* (Belle collaboration), Phys. Rev. D **100**, 031101 (2019), arXiv:1904.12093
[43] R. Aaij *et al.* (LHCb collaboration), Phys. Rev. D **102**, 071101(R) (2020), arXiv:2007.12096
[44] P. A. Zyla *et al.* (Particle Data Group), Prog. Theor. Exp. Phys. **2020**, 083C01 (2020)
[45] R. Aaij *et al.* (LHCb collaboration), JHEP **07**, 123 (2020), arXiv:2004.08163
[46] A. A. Alves Jr. *et al.* (LHCb collaboration), JINST **3**, S08005 (2008)
[47] R. Aaij *et al.* (LHCb collaboration), Int. J. Mod. Phys. A **30**, 1530022 (2015), arXiv:1412.6352
[48] R. Aaij *et al.*, JINST **9**, P09007 (2014), arXiv:1405.7808
[49] R. Arink *et al.*, JINST **9**, P01002 (2014), arXiv:1311.3893
[50] P. d 'Argent *et al.*, JINST **12**, P11016 (2017), arXiv:1708.00819
[51] M. Adinolfi *et al.*, Eur. Phys. J. C **73**, 2431 (2013), arXiv:1211.6759
[52] A. A. Alves Jr. *et al.*, JINST **8**, P02022 (2013), arXiv:1211.1346
[53] R. Aaij *et al.*, JINST **8**, P04022 (2013), arXiv:1211.3055
[54] T. Sjöstrand, S. Mrenna, and P. Skands, Comput. Phys. Commun. **178**, 852 (2008), arXiv: 0710.3820; T. Sjöstrand, S. Mrenna, and P. Skands, *PYTHIA 6.4 physics and manual*, JHEP **05**, 026 (2006), arXiv: hep-ph/0603175
[55] I. Belyaev *et al.*, J. Phys. Conf. Ser. **331**, 032047 (2011)
[56] D. J. Lange, Nucl. Instrum. Meth. A **462**, 152 (2001)
[57] N. Davidson, T. Przedzinski, and Z. Was, Comp. Phys. Comm. **199**, 86 (2016), arXiv:1011.0937
[58] S. Agostinelli *et al.* (Geant4 collaboration), Nucl. Instrum. Meth. A **506**, 250 (2003)
[59] M. Clemencic *et al.*, J. Phys. Conf. Ser. **331**, 032023 (2011)
[60] L. Breiman, J. H. Friedman, R. A. Olshen *et al.*, *Classification and regression trees*, (Wadsworth international group, Belmont, California, USA, 1984)
[61] Y. Freund and R. E. Schapire, J. Comput. Syst. Sci. **55**, 119 (1997)
[62] H. Voss, A. Hoecker, J. Stelzer *et al.*, PoS **ACAT** (2007) 040; A. Hoecker *et al.*, arXiv: physics/0703039
[63] G. Punzi, eConf **C030908** (2003) MODT002, arXiv: physics/0308063
[64] W. D. Hulsbergen, Nucl. Instrum. Meth. A **552**, 566 (2005), arXiv:physics/0503191
[65] T. Skwarnicki, *A study of the radiative cascade transitions between the Upsilon-prime and Upsilon resonances*, PhD

thesis, Institute of Nuclear Physics, Krakow, 1986, DESY-F31-86-02
[66] S. S. Wilks, Ann. Math. Stat. **9**, 60 (1938)
[67] E. Gross and O. Vitells, Eur. Phys. J. C **70**, 525 (2010), arXiv:1005.1891
[68] R. Aaij *et al.* (Geant4 collaboration), JINST **10**, P02007 (2015), arXiv:1408.1251
[69] L. Anderlini *et al.*, The PIDCalib package, LHCb-PUB-2016-021, (2016)
[70] R. Aaij *et al.*, Eur. Phys. J. Tech. Instr. **6**, 1 (2019), arXiv:1803.00824

R. Aaij[32] A.S.W. Abdelmotteleb[50] C. Abellan Beteta[44] F. Abudinén[50] T. Ackernley[54] B. Adeva[40] M. Adinolfi[48] H. Afsharnia[9] C. Agapopoulou[13] C.A. Aidala[76] S. Aiola[25] Z. Ajaltouni[9] S. Akar[59] K. Akiba[32] J. Albrecht[15] F. Alessio[42] M. Alexander[53] A. Alfonso Albero[39] Z. Aliouche[56] P. Alvarez Cartelle[49] S. Amato[2] J.L. Amey[48] Y. Amhis[11,42] L. An[42] L. Anderlini[22] M. Andersson[44] A. Andreianov[38] M. Andreotti[21] D. Andreou[62] D. Ao[6] F. Archilli[17] A. Artamonov[38] M. Artuso[62] E. Aslanides[10] M. Atzeni[44] B. Audurier[12] S. Bachmann[17] M. Bachmayer[43] J.J. Back[50] A. Bailly-reyre[13] P. Baladron Rodriguez[40] V. Balagura[12] W. Baldini[21] J. Baptista de Souza Leite[1] M. Barbetti[22,j] R.J. Barlow[56] S. Barsuk[11] W. Barter[55] M. Bartolini[49] F. Baryshnikov[38] J.M. Basels[14] G. Bassi[29,q] B. Batsukh[4] A. Battig[15] A. Bay[43] A. Beck[50] M. Becker[15] F. Bedeschi[29] I.B. Bediaga[1] A. Beiter[62] V. Belavin[38] S. Belin[40] V. Bellee[44] K. Belous[38] I. Belov[38] I. Belyaev[38] G. Bencivenni[23] E. Ben-Haim[13] A. Berezhnoy[38] R. Bernet[44] D. Berninghoff[17] H.C. Bernstein[62] C. Bertella[56] A. Bertolin[28] C. Betancourt[44] F. Betti[42] Ia. Bezshyiko[44] S. Bhasin[48] J. Bhom[35] L. Bian[67] M.S. Bieker[15] N.V. Biesuz[21] S. Bifani[47] P. Billoir[13] A. Biolchini[32] M. Birch[55] F.C.R. Bishop[49] A. Bitadze[56] A. Bizzeti M.P. Blago[49] T. Blake[50] F. Blanc[43] S. Blusk[62] D. Bobulska[53] J.A. Boelhauve[15] O. Boente Garcia[40] T. Boettcher[59] A. Boldyrev[38] N. Bondar[38,42] S. Borghi[56] M. Borsato[17] J.T. Borsuk[35] S.A. Bouchiba[43] T.J.V. Bowcock[54,42] A. Boyer[42] C. Bozzi[21] M.J. Bradley[55] S. Braun[60] A. Brea Rodriguez[40] J. Brodzicka[35] A. Brossa Gonzalo[50] D. Brundu[27] A. Buonaura[44] L. Buonincontri[28] A.T. Burke[56] C. Burr[42] A. Bursche[66] A. Butkevich[38] J.S. Butter[32] J. Buytaert[42] W. Byczynski[42] S. Cadeddu[27] H. Cai[67] R. Calabrese[21,i] L. Calefice[15,13] S. Cali[23] R. Calladine[47] M. Calvi[26,m] M. Calvo Gomez[74] P. Camargo Magalhaes[48] P. Campana[23] D.H. Campora Perez[73] A.F. Campoverde Quezada[6] S. Capelli[26,m] L. Capriotti[20,g] A. Carbone[20,g] G. Carboni[31] R. Cardinale[24,k] A. Cardini[27] I. Carli[4] P. Carniti[26,m] L. Carus[14] A. Casais Vidal[40] R. Caspary[17] G. Casse[54] M. Cattaneo[42] G. Cavallero[42] V. Cavallini[21,i] S. Celani[43] J. Cerasoli[10] D. Cervenkov[57] A.J. Chadwick[54] M.G. Chapman[48] M. Charles[13] Ph. Charpentier[42] C.A. Chavez Barajas[54] M. Chefdeville[8] C. Chen[3] S. Chen[4] A. Chernov[35] S. Chernyshenko[46] V. Chobanova[40] S. Cholak[43] M. Chrzaszcz[35] A. Chubykin[38] V. Chulikov[38] P. Ciambrone[23] M.F. Cicala[50] X. Cid Vidal[40] G. Ciezarek[42] G. Ciullo[i,21] P.E.L. Clarke[52] M. Clemencic[42] H.V. Cliff[49] J. Closier[42] J.L. Cobbledick[56] V. Coco[42] J.A.B. Coelho[11] J. Cogan[10] E. Cogneras[9] L. Cojocariu[37] P. Collins[42] T. Colombo[42] L. Congedo[19] A. Contu[27] N. Cooke[47] G. Coombs[53] I. Corredoira[40] G. Corti[42] B. Couturier[42] D.C. Craik[58] J. Crkovská[61] M. Cruz Torres[1,e] R. Currie[52] C.L. Da Silva[61] S. Dadabaev[38] L. Dai[65] E. Dall'Occo[15] J. Dalseno[40] C. D'Ambrosio[42] A. Danilina[38] P. d'Argent[15] J.E. Davies[56] A. Davis[56] O. De Aguiar Francisco[56] J. de Boer[42] K. De Bruyn[72] S. De Capua[56] M. De Cian[43] U. De Freitas Carneiro Da Graca[1] E. De Lucia[23] J.M. De Miranda[1] L. De Paula[2] M. De Serio[19,f] D. De Simone[44] P. De Simone[23] F. De Vellis[15] J.A. de Vries[73] C.T. Dean[61] F. Debernardis[19,f] D. Decamp[8] V. Dedu[10] L. Del Buono[13] B. Delaney[49] H.-P. Dembinski[15] V. Denysenko[44] O. Deschamps[9] F. Dettori[27,h] B. Dey[70] A. Di Cicco[23] P. Di Nezza[23] S. Didenko[38] L. Dieste Maronas[40] S. Ding[62] V. Dobishuk[46] A. Dolmatov[38] C. Dong[3] A.M. Donohoe[18] F. Dordei[27] A.C. dos Reis[1] L. Douglas[53] A.G. Downes[8] M.W. Dudek[35] L. Dufour[42] V. Duk[71] P. Durante[42] J.M. Durham[61] D. Dutta[56]

A. Dziurda[35] A. Dzyuba[38] S. Easo[51] U. Egede[63] V. Egorychev[38] S. Eidelman[38,†] S. Eisenhardt[52] S. Ek-In[43] L. Eklund[75] S. Ely[62] A. Ene[37] E. Epple[61] S. Escher[14] J. Eschle[44] S. Esen[44] T. Evans[56] L.N. Falcao[1] Y. Fan[6] B. Fang[67] S. Farry[54] D. Fazzini[26,m] M. Feo[42] A.D. Fernez[60] F. Ferrari[20] L. Ferreira Lopes[43] F. Ferreira Rodrigues[2] S. Ferreres Sole[32] M. Ferrillo[44] M. Ferro-Luzzi[42] S. Filippov[38] R.A. Fini[19] M. Fiorini[21,i] M. Firlej[34] K.M. Fischer[57] D.S. Fitzgerald[76] C. Fitzpatrick[56] T. Fiutowski[34] F. Fleuret[12] M. Fontana[13] F. Fontanelli[24,k] R. Forty[42] D. Foulds-Holt[49] V. Franco Lima[54] M. Franco Sevilla[60] M. Frank[42] E. Franzoso[21,i] G. Frau[17] C. Frei[42] D.A. Friday[53] J. Fu[6] Q. Fuehring[15] E. Gabriel[32] G. Galati[19,f] A. Gallas Torreira[40] D. Galli[20,g] S. Gambetta[52,42] Y. Gan[3] M. Gandelman[2] P. Gandini[25] Y. Gao[5] M. Garau[27,h] L.M. Garcia Martin[50] P. Garcia Moreno[39] J. García Pardiñas[26,m] B. Garcia Plana[40] F.A. Garcia Rosales[12] L. Garrido[39] C. Gaspar[42] R.E. Geertsema[32] D. Gerick[17] L.L. Gerken[15] E. Gersabeck[56] M. Gersabeck[56] T. Gershon[50] L. Giambastiani[28] V. Gibson[49] H.K. Giemza[36] A.L. Gilman[57] M. Giovannetti[23,t] A. Gioventù[40] P. Gironella Gironell[39] C. Giugliano[21,i] M.A. Giza[35] K. Gizdov[52] E.L. Gkougkousis[42] V.V. Gligorov[13,42] C. Göbel[64] E. Golobardes[74] D. Golubkov[38] A. Golutvin[55,38] A. Gomes[1,a] S. Gomez Fernandez[39] F. Goncalves Abrantes[57] M. Goncerz[35] G. Gong[3] I.V. Gorelov[38] C. Gotti[26] J.P. Grabowski[17] T. Grammatico[13] L.A. Granado Cardoso[42] E. Graugés[39] E. Graverini[43] G. Graziani A. T. Grecu[37] L.M. Greeven[32] N.A. Grieser[4] L. Grillo[53] S. Gromov[38] B.R. Gruberg Cazon[57] C. Gu[3] M. Guarise[21,i] M. Guittiere[11] P. A. Günther[17] E. Gushchin[38] A. Guth[14] Y. Guz[38] T. Gys[42] T. Hadavizadeh[63] G. Haefeli[43] C. Haen[42] J. Haimberger[42] S.C. Haines[49] T. Halewood-leagas[54] M.M. Halvorsen[42] P.M. Hamilton[60] J. Hammerich[54] Q. Han[7] X. Han[17] E.B. Hansen[56] S. Hansmann-Menzemer[17,42] L. Hao[6] N. Harnew[57] T. Harrison[54] C. Hasse[42] M. Hatch[42] J. He[6,c] K. Heijhoff[32] K. Heinicke[15] R.D.L. Henderson[63,50] A.M. Hennequin[58] K. Hennessy[54] L. Henry[42] J. Heuel[14] A. Hicheur[2] D. Hill[43] M. Hilton[56] S.E. Hollitt[15] R. Hou[7] Y. Hou[8] J. Hu[17] J. Hu[66] W. Hu[5] X. Hu[3] W. Huang[6] X. Huang[67] W. Hulsbergen[32] R.J. Hunter[50] M. Hushchyn[38] D. Hutchcroft[54] P. Ibis[15] M. Idzik[34] D. Ilin[38] P. Ilten[59] A. Inglessi[38] A. Iniukhin[38] A. Ishteev[38] K. Ivshin[38] R. Jacobsson[42] H. Jage[14] S.J. Jaimes Elles[41] S. Jakobsen[42] E. Jans[32] B.K. Jashal[41] A. Jawahery[60] V. Jevtic[15] X. Jiang[4,6] M. John[57] D. Johnson[58] C.R. Jones[49] T.P. Jones[50] B. Jost[42] N. Jurik[42] S. Kandybei[45] Y. Kang[3] M. Karacson[42] D. Karpenkov[38] M. Karpov[38] J.W. Kautz[59] F. Keizer[42] D.M. Keller[62] M. Kenzie[50] T. Ketel[33] B. Khanji[15] A. Kharisova[38] S. Kholodenko[38] T. Kirn[14] V.S. Kirsebom[43] O. Kitouni[58] S. Klaver[33] N. Kleijne[29,q] K. Klimaszewski[36] M.R. Kmiec[36] S. Koliiev[46] A. Kondybayeva[38] A. Konoplyannikov[38] P. Kopciewicz[34] R. Kopecna[17] P. Koppenburg[32] M. Korolev[38] I. Kostiuk[32,46] O. Kot[46] S. Kotriakhova A. Kozachuk[38] P. Kravchenko[38] L. Kravchuk[38] R.D. Krawczyk[42] M. Kreps[50] S. Kretzschmar[14] P. Krokovny[38] W. Krupa[34] W. Krzemien[36] J. Kubat[17] W. Kucewicz[35,34] M. Kucharczyk[35] V. Kudryavtsev[38] G.J. Kunde[61] D. Lacarrere[42] G. Lafferty[56] A. Lai[27] A. Lampis[27,h] D. Lancierini[44] J.J. Lane[56] R. Lane[48] G. Lanfranchi[23] C. Langenbruch[14] J. Langer[15] O. Lantwin[38] T. Latham[50] F. Lazzari[29,u] M. Lazzaroni[25,l] R. Le Gac[10] S.H. Lee[76] R. Lefèvre[9] A. Leflat[38] S. Legotin[38] P. Lenisa[i,21] O. Leroy[10] T. Lesiak[35] B. Leverington[17] H. Li[66] K. Li[7] P. Li[17] S. Li[7] Y. Li[4] Z. Li[62] X. Liang[62] C. Lin[6] T. Lin[51] R. Lindner[42] V. Lisovskyi[15] R. Litvinov[27,h] G. Liu[66] H. Liu[6] Q. Liu[6] S. Liu[4,6] A. Lobo Salvia[39] A. Loi[27] R. Lollini[71] J. Lomba Castro[40] I. Longstaff[53] J.H. Lopes[2] S. López Soliño[40] G.H. Lovell[49] Y. Lu[4,b] C. Lucarelli[22,j] D. Lucchesi[28,o] S. Luchuk[38] M. Lucio Martinez[32] V. Lukashenko[32,46] Y. Luo[3] A. Lupato[56] E. Luppi[21,i] A. Lusiani[29,q] K. Lynch[18] X.-R. Lyu[6] L. Ma[4] R. Ma[6] S. Maccolini[20] F. Machefert[11] F. Maciuc[37] V. Macko[43] P. Mackowiak[15] S. Maddrell-Mander[48] L.R. Madhan Mohan[48]

A. Maevskiy[38] D. Maisuzenko[38] M.W. Majewski[34] J.J. Malczewski[35] S. Malde[57] B. Malecki[35] A. Malinin[38] T. Maltsev[38] H. Malygina[17] G. Manca[27,h] G. Mancinelli[10] D. Manuzzi[20] C.A. Manzari[44] D. Marangotto[25,l] J.F. Marchand[8] U. Marconi[20] S. Mariani[22,j] C. Marin Benito[39] M. Marinangeli[43] J. Marks[17] A.M. Marshall[48] P.J. Marshall[54] G. Martelli[71,p] G. Martellotti[30] L. Martinazzoli[42,m] M. Martinelli[26,m] D. Martinez Santos[40] F. Martinez Vidal[41] A. Massafferri[1] M. Materok[14] R. Matev[42] A. Mathad[44] V. Matiunin[38] C. Matteuzzi[26] K.R. Mattioli[76] A. Mauri[32] E. Maurice[12] J. Mauricio[39] M. Mazurek[42] M. McCann[55] L. Mcconnell[18] T.H. McGrath[56] N.T. McHugh[53] A. McNab[56] R. McNulty[18] J.V. Mead[54] B. Meadows[59] G. Meier[15] D. Melnychuk[36] S. Meloni[26,m] M. Merk[32,73] A. Merli[25,l] L. Meyer Garcia[2] M. Mikhasenko[69,d] D.A. Milanes[68] E. Millard[50] M. Milovanovic[42] M.-N. Minard[8] A. Minotti[26,m] S.E. Mitchell[52] B. Mitreska[56] D.S. Mitzel[15] A. Mödden[15] R.A. Mohammed[57] R.D. Moise[55] S. Mokhnenko[38] T. Mombächer[40] I.A. Monroy[68] S. Monteil[9] M. Morandin[28] G. Morello[23] M.J. Morello[29,q] J. Moron[34] A.B. Morris[69] A.G. Morris[50] R. Mountain[62] H. Mu[3] F. Muheim[52] M. Mulder[72] K. Müller[44] C.H. Murphy[57] D. Murray[56] R. Murta[55] P. Muzzetto[27,h] P. Naik[48] T. Nakada[43] R. Nandakumar[51] T. Nanut[42] I. Nasteva[2] M. Needham[52] N. Neri[25,l] S. Neubert[69] N. Neufeld[42] P. Neustroev[38] R. Newcombe[55] E.M. Niel[43] S. Nieswand[14] N. Nikitin[38] N.S. Nolte[58] C. Normand[8,h,27] C. Nunez[76] A. Oblakowska-Mucha[34] V. Obraztsov[38] T. Oeser[14] D.P. O'Hanlon[48] S. Okamura[21,i] R. Oldeman[27,h] F. Oliva[52] M.E. Olivares[62] C.J.G. Onderwater[72] R.H. O'Neil[52] J.M. Otalora Goicochea[2] T. Ovsiannikova[38] P. Owen[44] A. Oyanguren[41] O. Ozcelik[52] K.O. Padeken[69] B. Pagare[50] P.R. Pais[42] T. Pajero[57] A. Palano[19] M. Palutan[23] Y. Pan[56] G. Panshin[38] A. Papanestis[51] M. Pappagallo[19,f] L.L. Pappalardo[21,i] C. Pappenheimer[59] W. Parker[60] C. Parkes[56] B. Passalacqua[21,i] G. Passaleva[22] A. Pastore[19] M. Patel[55] C. Patrignani[20,g] C.J. Pawley[73] A. Pearce[42] A. Pellegrino[32] M. Pepe Altarelli[42] S. Perazzini[20] D. Pereima[38] A. Pereiro Castro[40] P. Perret[9] M. Petric[53] K. Petridis[48] A. Petrolini[24,k] A. Petrov[38] S. Petrucci[52] M. Petruzzo[25] H. Pham[62] A. Philippov[38] R. Piandani[6] L. Pica[29,q] M. Piccini[71] B. Pietrzyk[8] G. Pietrzyk[11] M. Pili[57] D. Pinci[30] F. Pisani[42] M. Pizzichemi[26,m,42] V. Placinta[37] J. Plews[47] M. Plo Casasus[40] F. Polci[13,42] M. Poli Lener[23] M. Poliakova[62] A. Poluektov[10] N. Polukhina[38] I. Polyakov[62] E. Polycarpo[2] S. Ponce[42] D. Popov[6,42] S. Popov[38] S. Poslavskii[38] K. Prasanth[35] L. Promberger[42] C. Prouve[40] V. Pugatch[46] V. Puill[11] G. Punzi[29,r] H.R. Qi[3] W. Qian[6] N. Qin[3] S. Qu[3] R. Quagliani[43] N.V. Raab[18] R.I. Rabadan Trejo[6] B. Rachwal[34] J.H. Rademacker[48] R. Rajagopalan[62] M. Rama[29] M. Ramos Pernas[50] M.S. Rangel[2] F. Ratnikov[38] G. Raven[33,42] M. Rebollo De Miguel[41] F. Redi[42] F. Reiss[56] C. Remon Alepuz[41] Z. Ren[3] V. Renaudin[57] P.K. Resmi[10] R. Ribatti[29,q] A.M. Ricci[27] S. Ricciardi[51] K. Rinnert[54] P. Robbe[11] G. Robertson[52] A.B. Rodrigues[43] E. Rodrigues[54] J.A. Rodriguez Lopez[68] E. Rodriguez Rodriguez[40] A. Rollings[57] P. Roloff[42] V. Romanovskiy[38] M. Romero Lamas[40] A. Romero Vidal[40] J.D. Roth[76,†] M. Rotondo[23] M.S. Rudolph[62] T. Ruf[42] R.A. Ruiz Fernandez[40] J. Ruiz Vidal[41] A. Ryzhikov[38] J. Ryzka[34] J.J. Saborido Silva[40] N. Sagidova[38] N. Sahoo[47] B. Saitta[27,h] M. Salomoni[42] C. Sanchez Gras[32] I. Sanderswood[41] R. Santacesaria[30] C. Santamarina Rios[40] M. Santimaria[23] E. Santovetti[31,t] D. Saranin[38] G. Sarpis[14] M. Sarpis[69] A. Sarti[30] C. Satriano[30,s] A. Satta[31] M. Saur[15] D. Savrina[38] H. Sazak[9] L.G. Scantlebury Smead[57] A. Scarabotto[13] S. Schael[14] S. Scherl[54] M. Schiller[53] H. Schindler[42] M. Schmelling[16] B. Schmidt[42] S. Schmitt[14] O. Schneider[43] A. Schopper[42] M. Schubiger[32] S. Schulte[43] M.H. Schune[11] R. Schwemmer[42] B. Sciascia[23,42] A. Sciuccati[42] S. Sellam[40] A. Semennikov[38] M. Senghi Soares[33] A. Sergi[24,k] N. Serra[44] L. Sestini[28] A. Seuthe[15] Y. Shang[5] D.M. Shangase[76] M. Shapkin[38] I. Shchemerov[38] L. Shchutska[43] T. Shears[54] L. Shekhtman[38] Z. Shen[5] S. Sheng[4,6] V. Shevchenko[38] E.B. Shields[26,m] Y. Shimizu[11] E. Shmanin[38]

J.D. Shupperd[62] B.G. Siddi[21,i] R. Silva Coutinho[44] G. Simi[28] S. Simone[19,f] M. Singla[63] N. Skidmore[56] R. Skuza[17] T. Skwarnicki[62] M.W. Slater[47] I. Slazyk[21,i] J.C. Smallwood[57] J.G. Smeaton[49] E. Smith[44] M. Smith[55] A. Snoch[32] L. Soares Lavra[9] M.D. Sokoloff[59] F.J.P. Soler[53] A. Solomin[38,48] A. Solovev[38] I. Solovyev[38] F.L. Souza De Almeida[2] B. Souza De Paula[2] B. Spaan[15] E. Spadaro Norella[25,l] E. Spiridenkov[38] P. Spradlin[53] V. Sriskaran[42] F. Stagni[42] M. Stahl[59] S. Stahl[42] S. Stanislaus[57] O. Steinkamp[44] O. Stenyakin[38] H. Stevens[15] S. Stone[62] D. Strekalina[38] F. Suljik[57] J. Sun[27] L. Sun[67] Y. Sun[60] P. Svihra[56] P.N. Swallow[47] K. Swientek[34] A. Szabelski[36] T. Szumlak[34] M. Szymanski[42] S. Taneja[56] A.R. Tanner[48] M.D. Tat[57] A. Terentev[38] F. Teubert[42] E. Thomas[42] D.J.D. Thompson[47] K.A. Thomson[54] H. Tilquin[55] V. Tisserand[9] S. T'Jampens[8] M. Tobin[4] L. Tomassetti[21,i] G. Tonani[25,l] X. Tong[5] D. Torres Machado[1] D.Y. Tou[3] E. Trifonova[38] S.M. Trilov[48] C. Trippl[43] G. Tuci[6] A. Tully[43] N. Tuning[32,42] A. Ukleja[36] D.J. Unverzagt[17] E. Ursov[38] A. Usachov[32] A. Ustyuzhanin[38] U. Uwer[17] A. Vagner[38] V. Vagnoni[20] A. Valassi[42] G. Valenti[20] N. Valls Canudas[74] M. van Beuzekom[32] M. Van Dijk[43] H. Van Hecke[61] E. van Herwijnen[38] M. van Veghel[72] R. Vazquez Gomez[39] P. Vazquez Regueiro[40] C. Vázquez Sierra[42] S. Vecchi[21] J.J. Velthuis[48] M. Veltri[22,v] A. Venkateswaran[62] M. Veronesi[32] M. Vesterinen[50] D. Vieira[59] M. Vieites Diaz[43] X. Vilasis-Cardona[74] E. Vilella Figueras[54] A. Villa[20] P. Vincent[13] F.C. Volle[11] D. vom Bruch[10] A. Vorobyev[38] V. Vorobyev[38] N. Voropaev[38] K. Vos[73] R. Waldi[17] J. Walsh[29] C. Wang[17] J. Wang[5] J. Wang[4] J. Wang[3] J. Wang[67] M. Wang[5] R. Wang[48] Y. Wang[7] Z. Wang[44] Z. Wang[3] Z. Wang[6] J.A. Ward[50,63] N.K. Watson[47] D. Websdale[55] C. Weisser[58] B.D.C. Westhenry[48] D.J. White[56] M. Whitehead[53] A.R. Wiederhold[50] D. Wiedner[15] G. Wilkinson[57] M.K. Wilkinson[59] I. Williams[49] M. Williams[58] M.R.J. Williams[52] R. Williams[49] F.F. Wilson[51] W. Wislicki[36] M. Witek[35] L. Witola[17] C.P. Wong[61] G. Wormser[11] S.A. Wotton[49] H. Wu[62] K. Wyllie[42] Z. Xiang[6] D. Xiao[7] Y. Xie[7] A. Xu[5] J. Xu[6] L. Xu[3] M. Xu[50] Q. Xu[6] Z. Xu[9] Z. Xu[6] D. Yang[3] S. Yang[6] Y. Yang[6] Z. Yang[5] Z. Yang[60] L.E. Yeomans[54] H. Yin[7] J. Yu[65] X. Yuan[62] E. Zaffaroni[43] M. Zavertyaev[16] M. Zdybal[35] O. Zenaiev[42] M. Zeng[3] D. Zhang[7] L. Zhang[3] S. Zhang[65] S. Zhang[5] Y. Zhang[5] Y. Zhang[57] A. Zharkova[38] A. Zhelezov[17] Y. Zheng[6] T. Zhou[5] X. Zhou[6] Y. Zhou[6] V. Zhovkovska[11] X. Zhu[3] X. Zhu[7] Z. Zhu[6] V. Zhukov[14,38] Q. Zou[4,6] S. Zucchelli[20,g] D. Zuliani[28] G. Zunica[56]

(LHCb Collaboration)

[1]Centro Brasileiro de Pesquisas Físicas (CBPF), Rio de Janeiro, Brazil
[2]Universidade Federal do Rio de Janeiro (UFRJ), Rio de Janeiro, Brazil
[3]Center for High Energy Physics, Tsinghua University, Beijing, China
[4]Institute Of High Energy Physics (IHEP), Beijing, China
[5]School of Physics State Key Laboratory of Nuclear Physics and Technology, Peking University, Beijing, China
[6]University of Chinese Academy of Sciences, Beijing, China
[7]Institute of Particle Physics, Central China Normal University, Wuhan, Hubei, China
[8]Université Savoie Mont Blanc, CNRS, IN2P3-LAPP, Annecy, France
[9]Université Clermont Auvergne, CNRS/IN2P3, LPC, Clermont-Ferrand, France
[10]Aix Marseille Univ, CNRS/IN2P3, CPPM, Marseille, France
[11]Université Paris-Saclay, CNRS/IN2P3, IJCLab, Orsay, France
[12]Laboratoire Leprince-Ringuet, CNRS/IN2P3, Ecole Polytechnique, Institut Polytechnique de Paris, Palaiseau, France
[13]LPNHE, Sorbonne Université, Paris Diderot Sorbonne Paris Cité, CNRS/IN2P3, Paris, France
[14]I. Physikalisches Institut, RWTH Aachen University, Aachen, Germany
[15]Fakultät Physik, Technische Universität Dortmund, Dortmund, Germany
[16]Max-Planck-Institut für Kernphysik (MPIK), Heidelberg, Germany
[17]Physikalisches Institut, Ruprecht-Karls-Universität Heidelberg, Heidelberg, Germany
[18]School of Physics, University College Dublin, Dublin, Ireland
[19]INFN Sezione di Bari, Bari, Italy

[20]INFN Sezione di Bologna, Bologna, Italy
[21]INFN Sezione di Ferrara, Ferrara, Italy
[22]INFN Sezione di Firenze, Firenze, Italy
[23]INFN Laboratori Nazionali di Frascati, Frascati, Italy
[24]INFN Sezione di Genova, Genova, Italy
[25]INFN Sezione di Milano, Milano, Italy
[26]INFN Sezione di Milano-Bicocca, Milano, Italy
[27]INFN Sezione di Cagliari, Monserrato, Italy
[28]Università degli Studi di Padova, Università e INFN, Padova, Padova, Italy
[29]INFN Sezione di Pisa, Pisa, Italy
[30]INFN Sezione di Roma La Sapienza, Roma, Italy
[31]INFN Sezione di Roma Tor Vergata, Roma, Italy
[32]Nikhef National Institute for Subatomic Physics, Amsterdam, Netherlands
[33]Nikhef National Institute for Subatomic Physics and VU University Amsterdam, Amsterdam, Netherlands
[34]AGH - University of Science and Technology, Faculty of Physics and Applied Computer Science, Kraków, Poland
[35]Henryk Niewodniczanski Institute of Nuclear Physics Polish Academy of Sciences, Kraków, Poland
[36]National Center for Nuclear Research (NCBJ), Warsaw, Poland
[37]Horia Hulubei National Institute of Physics and Nuclear Engineering, Bucharest-Magurele, Romania
[38]Affiliated with an institute covered by a cooperation agreement with CERN
[39]ICCUB, Universitat de Barcelona, Barcelona, Spain
[40]Instituto Galego de Física de Altas Enerxías (IGFAE), Universidade de Santiago de Compostela, Santiago de Compostela, Spain
[41]Instituto de Fisica Corpuscular, Centro Mixto Universidad de Valencia - CSIC, Valencia, Spain
[42]European Organization for Nuclear Research (CERN), Geneva, Switzerland
[43]Institute of Physics, Ecole Polytechnique Fédérale de Lausanne (EPFL), Lausanne, Switzerland
[44]Physik-Institut, Universität Zürich, Zürich, Switzerland
[45]NSC Kharkiv Institute of Physics and Technology (NSC KIPT), Kharkiv, Ukraine
[46]Institute for Nuclear Research of the National Academy of Sciences (KINR), Kyiv, Ukraine
[47]University of Birmingham, Birmingham, United Kingdom
[48]H.H. Wills Physics Laboratory, University of Bristol, Bristol, United Kingdom
[49]Cavendish Laboratory, University of Cambridge, Cambridge, United Kingdom
[50]Department of Physics, University of Warwick, Coventry, United Kingdom
[51]STFC Rutherford Appleton Laboratory, Didcot, United Kingdom
[52]School of Physics and Astronomy, University of Edinburgh, Edinburgh, United Kingdom
[53]School of Physics and Astronomy, University of Glasgow, Glasgow, United Kingdom
[54]Oliver Lodge Laboratory, University of Liverpool, Liverpool, United Kingdom
[55]Imperial College London, London, United Kingdom
[56]Department of Physics and Astronomy, University of Manchester, Manchester, United Kingdom
[57]Department of Physics, University of Oxford, Oxford, United Kingdom
[58]Massachusetts Institute of Technology, Cambridge, MA, United States
[59]University of Cincinnati, Cincinnati, OH, United States
[60]University of Maryland, College Park, MD, United States
[61]Los Alamos National Laboratory (LANL), Los Alamos, NM, United States
[62]Syracuse University, Syracuse, NY, United States
[63]School of Physics and Astronomy, Monash University, Melbourne, Australia, associated to [50]
[64]Pontifícia Universidade Católica do Rio de Janeiro (PUC-Rio), Rio de Janeiro, Brazil, associated to [2]
[65]Physics and Micro Electronic College, Hunan University, Changsha City, China, associated to [7]
[66]Guangdong Provincial Key Laboratory of Nuclear Science, Guangdong-Hong Kong Joint Laboratory of Quantum Matter, Institute of Quantum Matter, South China Normal University, Guangzhou, China, associated to [3]
[67]School of Physics and Technology, Wuhan University, Wuhan, China, associated to [3]
[68]Departamento de Fisica , Universidad Nacional de Colombia, Bogota, Colombia, associated to [13]
[69]Universität Bonn - Helmholtz-Institut für Strahlen und Kernphysik, Bonn, Germany, associated to [17]
[70]Eotvos Lorand University, Budapest, Hungary, associated to [42]
[71]INFN Sezione di Perugia, Perugia, Italy, associated to [21]
[72]Van Swinderen Institute, University of Groningen, Groningen, Netherlands, associated to [32]
[73]Universiteit Maastricht, Maastricht, Netherlands, associated to [32]
[74]DS4DS, La Salle, Universitat Ramon Llull, Barcelona, Spain, associated to [39]
[75]Department of Physics and Astronomy, Uppsala University, Uppsala, Sweden, associated to [53]
[76]University of Michigan, Ann Arbor, MI, United States, associated to [62]
[a]Universidade Federal do Triângulo Mineiro (UFTM), Uberaba-MG, Brazil
[b]Central South U., Changsha, China
[c]Hangzhou Institute for Advanced Study, UCAS, Hangzhou, China
[d]Excellence Cluster ORIGINS, Munich, Germany
[e]Universidad Nacional Autónoma de Honduras, Tegucigalpa, Honduras
[f]Università di Bari, Bari, Italy
[g]Università di Bologna, Bologna, Italy
[h]Università di Cagliari, Cagliari, Italy
[i]Università di Ferrara, Ferrara, Italy
[j]Università di Firenze, Firenze, Italy

[k]Università di Genova, Genova, Italy
[l]Università degli Studi di Milano, Milano, Italy
[m]Università di Milano Bicocca, Milano, Italy
[n]Università di Modena e Reggio Emilia, Modena, Italy
[o]Università di Padova, Padova, Italy
[p]Università di Perugia, Perugia, Italy
[q]Scuola Normale Superiore, Pisa, Italy
[r]Università di Pisa, Pisa, Italy
[s]Università della Basilicata, Potenza, Italy
[t]Università di Roma Tor Vergata, Roma, Italy
[u]Università di Siena, Siena, Italy
[v]Università di Urbino, Urbino, Italy

[†]Deceased